0026-895X/90/030348-09$02.00/0

MOLECULAR PHARMACOLOGY, 38:348-356

p-[^{125}I]Iodoclonidine, a Novel Radiolabeled Agonist for Studying Central α_2-Adrenergic Receptors

BRUCE M. BARON and BARRY W. SIEGEL
Merrell Dow Research Institute, Cincinnati, Ohio 45215
Received October 6, 1989; Accepted June 5, 1990

SUMMARY

Unlabeled *p*-iodoclonidine was efficacious in attenuating forskolin-stimulated cAMP accumulation in SK-N-SH neuroblastoma cells. Maximal attenuation was 76 ± 3%, with an EC_{50} of 347 ± 60 nM. Comparable values of epinephrine were 72 ± 3% and 122 ± 22 nM. Responses to both agonists were abolished by 10 μM phentolamine. Therefore, *p*-iodoclonidine is an agonist in a cell culture model system of the neuronal α_2-adrenergic receptor. *p*-[^{125}I]Iodoclonidine binding to membranes were measured using various regions of the rat brain. The agonist labeled a single population of sites present on cerebral cortical membranes, which was saturable (B_{max} = 230 fmol/mg of protein) and possessed high affinity for the ligand (K_d = 0.6 nM). Binding was largely specific (93% at 0.6 nM). A variety of α_2-adrenergic agonists and antagonists were shown to compete for the binding of the radioligand. The binding of *p*-[^{125}I]iodoclonidine was much less sensitive to agents that interact with α_1-adrenergic, serotonergic, and dopaminergic receptors. Approximately 65% of the binding was sensitive to guanine nucleotides. Association kinetics using 0.4 nM radioligand were biphasic (37% associate rapidly, with k_{obs} = 0.96 min^{-1}, with the remainder binding more slowly, with k_{obs} = 0.031 min^{-1}) and reached a plateau by 90 min at 25°. Dissociation kinetics were also biphasic, with 30% of the binding dissociating rapidly (k_1 = 0.32 min^{-1}) and the remainder dissociating 50-fold more slowly (k_2 = 0.006 min^{-1}). Agonist binding is, therefore, uniquely complex and probably reflects the conformational changes that accompany receptor activation.

α_2ARs are present in the mammalian central nervous system, where they mediate a variety of biochemical and electrophysiological responses (1). As in nonneuronal tissues, neuronal α_2ARs are coupled to attenuation of the second messenger-producing enzyme adenylate cyclase (2–5). Paradoxically, under certain conditions, α_2AR occupation can synergistically increase cAMP production elicited by nonadrenergic stimuli (6, 7). Several of the biochemical sequelae of neuronal α_2AR activation also may occur independently of these changes in cAMP levels. For example, α_2AR agonists attenuate neurotransmitter release from isolated atrial (8, 9) and cortical slice preparations (10), even when the capacity to reduce cellular cAMP content is blocked enzymatically with pertussis toxin pretreatment or by artificial elevation of second messenger concentrations using cell-permeable cAMP analogs. It is not, at present, clear whether these distinct biochemical events are mediated by a single type of neurotransmitter recognition site or, instead, whether a distinct protein species is preferentially associated with each biochemical response. Support for the existence of α_2AR subtypes comes from several sources. There are at least three α_2AR gene products (11, 12). Expression and transfection of two such clones reveal dramatically different ligand binding profiles (13). These results are consistent with earlier pharmacological classifications of α_2ARs obtained from naturally occurring tissue sources. For example, receptor binding measurements have identified ligands that appear to bind with some selectivity to receptors obtained from different tissue sources (14). Finally, it has been suggested that certain compounds have a selective ability to block or activate presynaptic versus postsynaptic α_2ARs (15, 16).

A current problem in the measurement of drug interactions with neuronal α_2AR subtypes is the lack of a radioligand that combines high specific activity with low nonspecific binding to permit the use of discrete brain regions or cultured cell model systems as convenient sources of membrane preparations. Recently, however, Van Dort *et al.* (17) reported the preparation of an iodinated derivative of the α_2AR agonist clonidine. They demonstrated that this compound, *p*-iodoclonidine, inhibited the binding of *p*-[^{3}H]aminoclonidine to human platelet α_2ARs with nanomolar affinity. We report here the binding characteristics of *p*-[^{125}I]iodoclonidine to rat brain membranes and demonstrate the utility of this radioligand for studying drug-receptor interactions in discrete brain regions.

Materials and Methods

Membrane preparation. Receptor binding studies employed a crude synaptosomal membrane preparation that was extensively

ABBREVIATIONS: α_2AR, α_2-adrenergic receptor; HEPES, 4-(2-hydroxyethyl)-1-piperazineethanesulfonic acid; EGTA, ethylene glycol bis(β-aminoethyl ether)-*N*,*N*,*N*′,*N*′-tetraacetic acid; α_1AR, α_1-adrenergic receptor; GTPγS, guanosine-5′-*O*-(3-thio)triphosphate; GDPβS, guanosine-5′-*O*-(2-thiol)diphosphate; Gpp(NH)p, guanosine-5′-(2,3-imido)triphosphate.

washed to remove endogenous guanine nucleotides. Previously, Neubig and Szamraj (18) have shown the importance of guanine nucleotide removal on the observed levels of agonist binding. We have encountered similar problems in our studies of central nervous system glutamate receptors and have utilized a Triton lysis procedure, as described by Baron *et al.* (19), to remove endogenous amino acid stores. This membrane preparation also proved to be suitable for p-[^{125}I]iodoclonidine binding and was used throughout these studies. Briefly, male Sprague Dawley rats (150–250 g; Charles River) were killed by decapitation and the cerebral cortex and hippocampus were removed, combined, and homogenized in 15 volumes of ice-cold 0.32 M sucrose, using a Teflon-glass homogenizer. Unless specified, all further manipulations were performed at 4°. Following centrifugation (1000 × *g*, 10 min), the supernatants were collected and centrifuged (44,000 × *g*, 20 min). The supernatant was aspirated and discarded and the buffy layer of each pellet was resuspended in 15 volumes of ice-cold H_2O and homogenized using a Brinkman Polytron (setting 6, 10 sec). These membranes were washed once in distilled H_2O, followed by resuspension of the buffy layer in 5 volumes of distilled H_2O. This membrane suspension was then subjected to two 5-min freeze-thaw cycles using a dry ice-methanol bath. The volume was adjusted to 15 volumes with distilled H_2O and the suspension was centrifuged as above. Pellets were resuspended in 5 volumes of 10 mM HEPES-KOH, pH 7.4, containing 0.04% (v/v) Triton X-100 and were incubated at 37° for 15 min. The volume was adjusted to 15 volumes with 10 mM HEPES-KOH (pH 7.4) and the membranes were washed three times at 4°. The final pellets were pooled in 3 volumes of 10 mM HEPES-KOH (pH 7.4) and stored at −80° in aliquots. On the day of assay, membrane aliquots were thawed at room temperature, resuspended in 30 ml of 50 mM Tris·HCl (pH 7.6 at 25°) containing 10 mM $MgCl_2$, incubated 15 min at 37°, and then centrifuged at 44,000 × *g* for 20 min. This washing procedure was repeated twice and then the final membrane pellet was resuspended in 3 volumes of 50 mM Tris·HCl (pH 7.6), 10 mM $MgCl_2$, 1 mM EGTA (buffer A).

Protein was measured using a dye binding method, according to the manufacturers directions (Bio-Rad).

Radioligand binding assays. p-[^{125}I]Iodoclonidine (2200 Ci/mmol) was generously provided by Dr. Russell Garlick (Dupont New England Nuclear) as a stock solution in ethanol. Immediately before use, the required volume of the radioligand was withdrawn, evaporated to dryness *in vacuo*, and resuspended as a 5× stock in buffer A. Assays were conducted in 12 × 75 mm polypropylene tubes. Each assay tube (final volume, 50 μl) contained 10 μl of radioligand, 20 μl of buffer A containing any unlabeled drugs or nucleotides, and 20 μl of membranes (20–50 μg of protein). Nonspecific binding was defined using 10 μM phentolamine. Assays were initiated by membrane addition and then transferred to a 25° shaking water bath. In equilibrium binding experiments, the incubation time was 90 min. Assays were terminated by addition of 4 ml of ice-cold wash buffer (50 mM Tris·HCl, pH 7.6, 10 mM $MgCl_2$), followed by filtration through GF/B filter strips. Filters were washed two times with 4 ml of cold buffer and then transferred to polystyrene tubes for measurement of radioactivity, using a Packard Cobra Auto-Gamma Counter. Unlabeled drugs were obtained as follows: UK 14,304 tartrate and prazosin hydrochloride, Pfizer Inc.; BHT 920 hydrochloride, Boehringer Ingelheim; oxymetazoline hydrochloride, E. Merck; rauwolscine hydrochloride, Roth; piperoxan hydrochloride, Rhone Poulenc; p-iodoclonidine hydrochloride and mianserin hydrochloride, Research Biochemicals; phentolamine hydrochloride, Ciba Geigy; dihydroergocryptine methane sulfonate, Chemodyne S.A.; and WB 4101 hydrochloride, WB Pharmaceuticals, Ltd. Idazoxan hydrochloride and clonidine hydrochloride were synthesized at Merrell Dow Research Institute. All other drugs and reagents were obtained from Sigma Chemical Co.

[^{3}H]Rauwolscine (86–88 Ci/mmol; DuPont New England Nuclear) binding was assessed as described by Cheung *et al.* (20). Unless specified, we employed the same membrane preparation as used for p-[^{125}I] iodoclonidine binding, to enable side by side comparisons of the binding properties of agonist and antagonist radioligands. On the day of assay, the membranes were thawed, resuspended in 50 mM Tris·HCl, pH 7.5, containing 0.5 mM EDTA and 0.1% ascorbic acid, and washed twice in the same buffer. Assays were performed in triplicate and contained 300 μg of membrane protein, various concentrations of unlabeled test compounds, and [^{3}H]rauwolscine (1 nM for competition binding experiments and 2 to 1000 nM for saturation binding experiments). Following a 60-min incubation at 25°, assays were terminated by filtration. Nonspecific binding was defined using 1 μM unlabeled yohimbine.

Kinetic studies. Association and dissociation experiments employed several-milliliter volumes of starting reaction mixtures of the same volume ratios (10 parts radioligand, 20 parts buffer containing any additions, and 20 parts membranes) as in equilibrium binding experiments. The experiments described below utilized 0.4 nM radioligand. Separate incubations were performed to measure kinetics of nonspecific binding. In dissociation experiments, dissociation was initiated by addition of appropriate volumes of a 100 × stock of unlabeled drug (phentolamine or in some cases epinephrine) or by a 100-fold dilution into 25° buffer. Epinephrine-induced dissociation experiments included 0.02% ascorbate. Aliquots were withdrawn from the reaction mixture at various times, combined with 4 ml of cold wash buffer, and filtered through 24-mm-diameter GF/B glass fiber filters. Filters were immediately washed with two 4-ml portions of cold wash buffer.

α_2AR-mediated attenuation of cyclic AMP accumulation. Agonist activity at neuronal α_2AR was measured by the ability of p-iodoclonidine and epinephrine to attenuate forskolin (1 μM)-stimulated cAMP accumulation in SK-N-SH neuroblastoma cells. Methods of cell culture and cAMP determination were as described by Baron and Siegel (5), with the exception that the present experiments utilized cells of passages 141 to 144, the neuroblastoma cells were pretreated with 100 μM pargyline, and all assay tubes contained, in addition, 0.02% ascorbic acid. Results are expressed as the percentage of attenuation of forskolin-stimulated cAMP accumulation observed in the presence of the α_2-adrenergic agonist.

Data analysis. Data were analyzed using programs written in RS/1, version 4.01 (BBN Software Products), and run on a VAX computer system. Receptor binding and functional response data were plotted as percentage of inhibition (competition binding experiments and cAMP attenuation measurements) or amount bound (saturation binding experiments) versus the logarithm of the test drug concentration and were fit using nonlinear regression analysis. Equilibrium binding data were fit to a logistic function of the form: $f(x) = BX + M(X^n)/(K^n + X^n)$, where B is the observed dependence of nonspecific binding on radioligand concentration (obtained by fitting nonspecific binding data to $f(x) = BX$; B is fixed at 0 for inhibition data), M is the calculated maximal response (e.g., a variable representing the B_{max} in saturation studies, maximal stimulation of binding in experiments utilizing divalent cations, or maximal attenuation of cAMP accumulation in functional assays but fixed at 100 in competition experiments), X is the concentration of the test drug, K is the apparent affinity of the test drug (e.g., K_d in saturation experiments and IC_{50} in competition experiments), and n is a slope factor ($n = 1$ in saturation experiments). In certain cases, inhibition data were modeled to an equation specifying either a "floating" or a "fixed" maximal inhibition by allowing M to vary (floating) or by setting $M = 100$ (fixed). In both models the slope factor, n, was 1. Statistical testing of the appropriateness of particular models was performed using the F ratio statistic, calculated using the "extra sum of squares principle" described by Munson and Rodbard (21). Association experiments were analyzed by fitting specific binding data to the equation: $f(t) = B_{eq}(1 - Ae^{-k_1 t} - (1 - A)e^{-k_2 t})$, where B_{eq} is the binding at infinite time (e.g., equilibrium), k_1 and k_2 are kinetic constants, and A is the fraction of sites with kinetic constant equal to k_1. The value of A was set to 0 for single-exponential association but was allowed to vary for a double-exponential model. Dissociation experiments were analyzed by fitting specific binding data to the following equation: $f(t) = B_0[Ae^{-k_1 t} + (1 - A)e^{-k_2 t}]$, where B_0 is the binding before initiation of dissociation, k_1 and k_2 are kinetic constants, and A, the fraction with kinetic constant equal to k_1, is set to 1 for

single-exponential dissociation and allowed to vary for double-exponential dissociation.

Results

Effects of *p*-iodoclonidine on cAMP accumulation. Epinephrine and unlabeled *p*-iodoclonidine were compared for their ability to attenuate for forskolin-stimulated cAMP accumulation in SK-N-SH neuroblastoma cells (5). Forskolin (1 μM) elicited a 4.6- ± 0.7-fold change in cAMP levels in SK-N-SH cells (three experiments). As shown in Fig. 1, both epinephrine and *p*-iodoclonidine were able to attenuate the response to forskolin. EC_{50} values were 124 ± 22 nM and 347 ± 60 nM, respectively (three experiments). The two agonists achieved similar maximal effects on cAMP accumulation (72 ± 3% and 76 ± 3%, respectively; three experiments). Phentolamine (10 μM) completely antagonized the response to both agonists.

Saturation binding of *p*-[^{125}I]iodoclonidine. Various concentrations of *p*-[^{125}I]iodoclonidine were incubated with well washed brain membranes for 90 min at 25°. Preliminary experiments had demonstrated that maximal levels of specific binding are obtained at this time point. Fig. 2A demonstrates that *p*-[^{125}I]iodoclonidine binding is specific, saturable, and of high affinity. Transformation by the method of Scatchard (22) resulted in a straight line, consistent with the radioligand interacting with a single class of binding sites (Fig. 2B). k_d and B_{max} values were 0.55 ± 0.07 nM and 230 ± 38 fmol/mg of protein, respectively (three experiments). Specific binding at radioligand concentrations approximating the K_d (0.6 nM) accounted for 92.5 ± 1.6% of the total binding (three experiments).

The relative density of agonist and antagonist binding sites was assessed in subsequent experiments by comparing saturation binding isotherms obtained using *p*-[^{125}I]iodoclonidine and [^{3}H]rauwolscine, respectively. Under these conditions, the agonist labeled 45% of the total antagonist binding sites. Respective K_d values were 0.68 ± 0.01 and 12.8 ± 0.2 nM and B_{max} values were 166 ± 9 and 370 ± 38 fmol/mg of protein (three experiments).

Structure-activity studies of *p*-[^{125}I]iodoclonidine binding. A number of α_2-adrenergic agonists and antagonists were tested for their ability to compete for the binding of *p*-[^{125}I]iodoclonidine to α_2ARs present on brain membranes (Table 1). Generally, agonists were more potent than antagonists in competing for binding. The most potent agonist competitors possessed an imidazoline group (e.g., UK 14,304, oxymetazoline, and clonidine). BHT 920, which possesses a structurally similar thiazole ring, was also very potent in this assay. However, neither was an imidazoline moiety necessary (e.g., the catecholamines epinephrine and norepinephrine) nor was an imidazole group sufficient (cimetidine, 3 ± 2% inhibition at 10 μM) for potent binding. Catecholamines could compete for 100% of the binding of the radioligand, with a rank order of potency equal to epinephrine > norepinephrine > dopamine > serotonin (Fig. 3). Consistent with the binding sites being α-adrenergic in nature was the ineffectiveness of the β-adrenergic antagonist propranolol (IC_{50} = 88 ± 18 μM). The most potent antagonist competitors also possessed an imidazoline moiety (e.g., phentolamine and idazoxan) but, again, this was not essential because both dihydroergocryptine and mianserin lack this heterocycle but were also very potent. Interestingly, it is

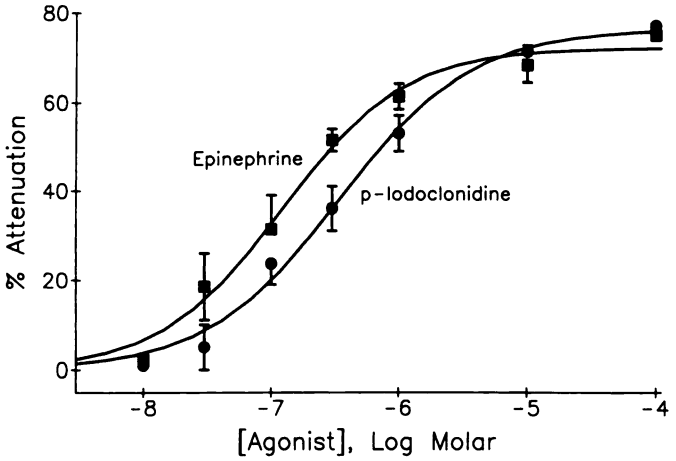

Fig. 1. α_2AR-mediated attenuation of cAMP accumulation in SK-N-SH human neuroblastoma cells. Inhibition of forskolin-stimulated (1 μM) cyclic AMP accumulation was measured in suspended SK-N-SH cells previously labeled with [^{3}H]adenine. Results shown are means ± standard errors of three separate experiments. ——, Computer-generated curves, as described in the text. In these experiments, basal conversion of cell-associated radioactivity to cAMP was 0.13 ± 0.02%, with forskolin elevating this conversion to 0.59 ± 0.07%. *Abscissa*, percentage of attenuation of the forskolin response, with the basal value representing 100% attenuation.

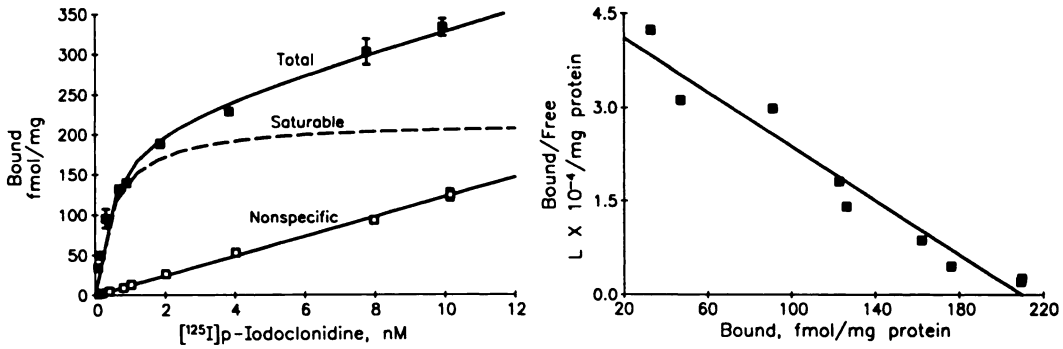

Fig. 2. Saturation binding of *p*-[^{125}I]iodoclonidine binding to rat brain membranes. Well washed pooled hippocampal plus cortical membranes were incubated with various concentrations of *p*-[^{125}I]iodoclonidine in the absence (total binding) or presence of 10 μM phentolamine (nonspecific binding). A, Total binding (■) and nonspecific binding (□) are calculated as fmol/mg of protein and plotted versus radioligand concentration (nM), as means ± standard errors of quadruplicate determinations from a single experiment repeated twice. *Error bars* are not displayed where smaller than the *symbols*. *Solid lines connecting total binding and nonspecific binding*, the computer-generated fit to the equations $f(x) = BX + MXI(K + X)$ and $f(x) = BX$, respectively. – – –, Curve of predicted specific binding equal to total − nonspecific. B, Scatchard transformation of the data shown in A. ——, Best fit line to the experimental points.

TABLE 1

Inhibition of p-[125I]iodoclonidine binding by selected compounds

Inhibition of the binding of 0.4 nM p-[125I]iodoclonidine was measured in the presence of seven to nine concentrations of unlabeled test compounds. Specific binding was defined using 10 μM phentolamine. Results were modeled using the equation $f(x) = 100X^n/(K^n + X^n)$, where X = concentration of unlabeled ligand, n = slope factor, and K = IC_{50} value. Results are means ± standard errors for three experiments.

	IC_{50}	Slope factor
	nM	
(−)-Epinephrine	13 ± 2	0.92 ± 0.05
(−)-Norepinephrine	21 ± 2	0.74 ± 0.05[a]
Serotonin	63,000 ± 8,000	1.75 ± 0.06[a]
Dopamine	263 ± 14	0.72 ± 0.07
Oxymetazoline	3 ± 0	0.99 ± 0.04
Clonidine	3 ± 0	0.77 ± 0.02[a]
UK 14,304	3 ± 0	0.91 ± 0.10
Phenylephrine	169 ± 21	0.79 ± 0.03[a]
BHT 920	19 ± 2	0.75 ± 0.06
Idazoxan	21 ± 1	0.92 ± 0.05
Phentolamine	21 ± 2	0.73 ± 0.08
RS 21,361	4,200 ± 300	0.80 ± 0.02[a]
Yohimbine	229 ± 16	0.88 ± 0.06
Corynanthine	106,000 ± 48,000	0.79 ± 0.07
Rauwolscine	391 ± 62	0.74 ± 0.05[a]
Piperoxan	233 ± 10	0.96 ± 0.06
Mianserin	138 ± 10	0.97 ± 0.06
Dihydroergocryptine	28 ± 6	0.88 ± 0.04
(+)-LSD[b]	27 ± 1	0.97 ± 0.04
(−)-LSD	116,000 ± 4,000	0.91 ± 0.09
WB 4,101	1,155 ± 107	0.84 ± 0.05
Prazosin	42,000 ± 700	0.64 ± 0.10[a]

[a] $p < 0.05$ different than unity, two tailed t test.
[b] LSD, lysergic acid diethylamide.

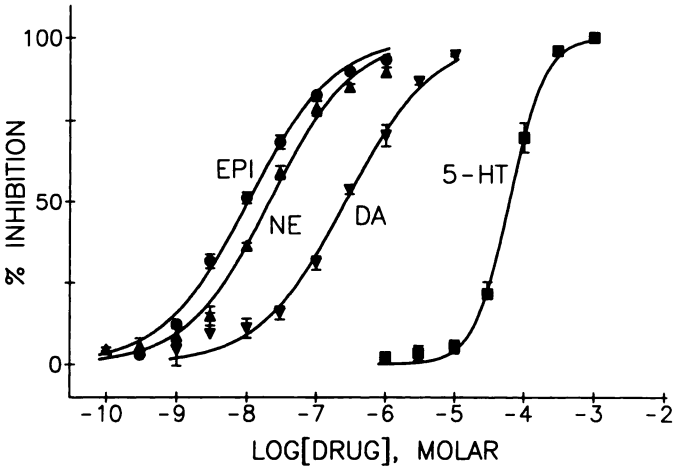

Fig. 3. Inhibition of p-[125I]iodoclonidine binding by biogenic amine neurotransmitters. The inhibition of the specific binding of 0.4 nM radioligand was measured in the presence of various concentrations of epinephrine (*EPI*) (●), norepinephrine (*NE*) (▲), serotonin (*5-HT*) (■), or dopamine (DA) (▼). Data points are means ± standard errors of three experiments. ——, Computer-generated fit to $f(x) = 100X^n/(K^n + X^n)$. *Error bars* are omitted where smaller than the *symbols*.

the ergot portion of dihydroergocryptine that is responsible for its α_2-adrenergic antagonism. Replacement of the peptide portion of dihydroergocryptine with two ethyl groups, as in lysergic acid diethylamide, is without effect on potency. Moreover, lysergic acid diethylamide binds to the α_2AR in a stereoselective fashion, with the (+)-isomer being 4000-fold more potent than the (−)-isomer. Yohimbine and rauwolscine, which like dihydroergocryptine contain large planar hydrophobic substituents, were less potent. At sufficiently high concentrations, these

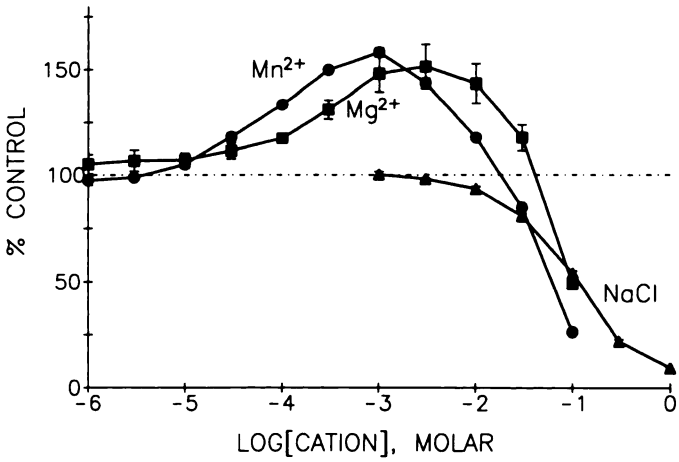

Fig. 4. Modulation of p-[125I]iodoclonidine binding by inorganic cations. Specific binding of 0.4 nM radioligand was measured in the presence of various concentrations of $MnCl_2$ (●), $MgCl_2$ (■), or NaCl (▲). Data points are means ± standard errors of three experiments. *Error bars* are omitted where smaller than the *symbols*.

compounds could compete for 100% of the binding of the labeled ligand. The α_1AR-preferring stereoisomer of yohimbine, corynanthine, was more than 2 orders of magnitude less potent. Idazoxan, in addition to the previously discussed imidazoline group, contains a benzodioxane moiety. Therefore, we compared two benzodioxane-containing drugs, piperoxan and WB 4,101. The former compound, a mixed α_1-α_2 antagonist, inhibited binding with potency similar to that of yohimbine, whereas WB 4,101, an α_1AR-preferring antagonist, required micromolar concentrations. Also underscoring the importance of the nitrogen-containing heterocycle is the effect of substitution of an imidazoline group with less basic imidazole group. RS 21,361, an imidazole analog of idazoxan, was approximately 200-fold less potent than the parent compound.

We considered the possibility that the relatively low affinity of antagonists (e.g., yohimbine and rauwolscine), compared with that of agonists (e.g., epinephrine and UK 14,304), might be related to our method of membrane preparation. Therefore, we compared [3H]rauwolscine binding and p-[125I]iodoclonidine binding to a P_2 membrane fraction [prepared according to the method of Cheung *et al.* (20)] with those results obtained with the Triton-washed membrane preparation. Yohimbine and UK 14,304 affinities for p-[125I]iodoclonidine binding sites were similar in the P_2 fraction and Triton-washed membranes. IC_{50} values were 427 ± 206 and 229 ± 16 nM (yohimbine) and 6.7 ± 3.1 and 3 ± 0 nM (UK 14,304) in the P_2 fraction and Triton-washed membranes, respectively, Moreover, IC_{50} values for yohimbine versus [3H]rauwolscine were similar in crude and well washed membranes (22 ± 1 and 18 ± 2 nM, respectively). Epinephrine and p-iodoclonidine inhibition of [3H]rauwolscine binding to crude membranes was characterized by shallow slopes (slope factors of 0.74 ± 0.04 and 0.56 ± 0.06, respectively) and IC_{50} values (590 ± 184 and 51 ± 10 nM, respectively) at least 1 order of magnitude greater than those obtained using p-[125I]iodoclonidine binding.

Binding was also regulated by inorganic ions (Fig. 4). Sodium ions could inhibit 100% of the binding of the radiolabeled agonist (IC_{50} = 109 ± 2 mM), with a slope factor not different than unity (1.15 ± 0.05). In contrast, the divalent cations magnesium and manganese enhanced the binding of the agonist by 46 ± 3 and 61 ± 3%, respectively. Both metal ions exhibited

TABLE 2

Comparison of alternative models describing nucleotide inhibition of p-[^{125}I]iodoclonidine binding

Competition binding data were modeled to either $f(x) = MX^n/(K^n + X^n)$ (floating model) or $f(x) = 100X^n/(K^n + X^n)$ (fixed model), where X = concentration of unlabeled ligand, $K = IC_{50}$ value, M = maximal inhibition value, and n = slope factor. Appropriateness of individual models was evaluated statistically by comparing residual sum of squares values according to the method of Munson and Rodbard (21). An IC_{50} was not achieved using ATP, which gave 22 ± 2% inhibition at 1 mM.

Nucleotide	Fixed model		Float model		
	IC_{50}	Slope	IC_{50}	Maximal inhibition	Slope
	$\times 10^{-6}$ M		$\times 10^{-6}$ M	Percent	
GTP	58.1 ± 16.0	0.51 ± 0.08	35.2 ± 9.9	90 ± 5	0.57 ± 0.05[a]
GDP	133.0 ± 27.7	0.63 ± 0.08	35.4 ± 1.4	72 ± 1	1.07 ± 0.03
GMP	1079 ± 299	0.89 ± 0.05	ND[b]	ND	ND
GDPβS	13.1 ± 6.4	0.22 ± 0.07	0.36 ± 0.09	61 ± 2	0.94 ± 0.20[a]
Gpp(NH)p	13.8 ± 3.8	0.12 ± 0.00	3.3 ± 14.1	92 ± 26	0.12 ± 0.04[a]
GTPγS	1.6 ± 0.4	0.25 ± 0.13	0.06 ± 0.05	76 ± 9	0.39 ± 0.09[a]

[a] Floating model is preferred ($p < 0.05$).
[b] ND, not determined.

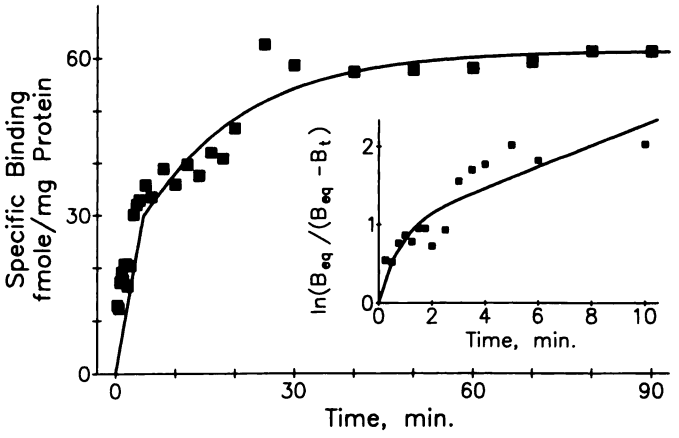

Fig. 5. Association kinetics of p-[^{125}I]iodoclonidine. Membranes were incubated with 0.4 nM radioligand in the presence or absence of 10 μM phentolamine. Samples were withdrawn at various time intervals and bound ligand was determined. Results are expressed as specific binding (fmol/mg of protein) at each time point. Data shown are from a single experiment conducted in duplicate and repeated twice. ——, Computer-generated line for the equation:

$$f(t) = B_{eq}(1 - Ae^{-k_1 t} - (1 - A)e^{-k_2 t})$$

where B_{eq} is the binding at infinite time, k_1 and k_2 are association constants, A is the fraction of sites with kinetic constant k_1, and t is time. *Inset*, transformation of the same data (first 10 min only) as $\ln[B_{eq}/(B_{eq} - B_t)]$ versus time. ——, Data modeled to the double-exponential equation and then subjected to the same transformation.

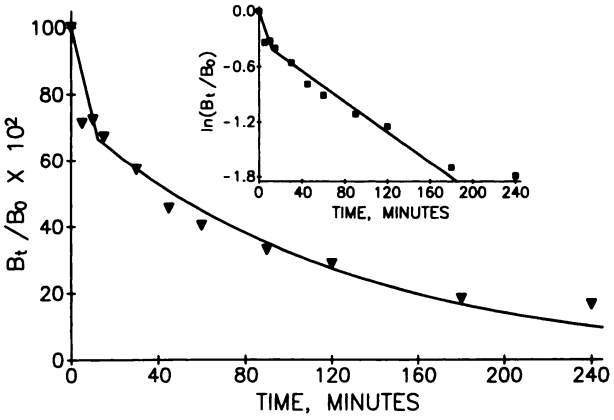

Fig. 6. Dissociation kinetics of p-[^{125}I]iodoclonidine. Membranes were incubated with 0.4 nM radioligand in the presence or absence of 10 μM phentolamine for 90 min at 25°. Samples were withdrawn for determination of binding at t_0 (i.e., B_0), and then dissociation was initiated by phentolamine addition to the control membranes. Samples were withdrawn periodically to determine bound ligand at time t (i.e., B_t). The fraction remaining (B_t/B_0) is plotted versus time. ——, Computer-generated fit to the double-exponential equation:

$$f(t) = B_0[Ae^{-k_1 t} + (1 - A)e^{-k_2 t}]$$

where A is the fraction of sites with dissociation constant of k_1 (the remainder of constant k_2). Results are from a single experiment conducted in duplicate and repeated three times. *Inset*, semilogarithmic plot of the same data.

biphasic concentration-response curves, enhancing binding at low concentrations and inhibiting it at higher concentrations. For calculations, we focused on the rising phase of the curve and excluded values in the inhibitory phase. In addition to being more efficacious, Mn^{2+} was also more potent. EC_{50} values were 79 ± 9 (Mn^{2+}) and 191 ± 14 μM (Mg^{2+}). Magnesium (0.1 to 100 mM) had the opposite effect on [^{3}H]rauwolscine binding, inhibiting binding with an IC_{50} of 46 mM (data not shown).

Guanine nucleotide effects on p-[^{125}I]iodoclonidine binding. A variety of guanine nucleotides and their analogs were tested for their ability to influence the steady state binding of p-[^{125}I]iodoclonidine. These data are summarized in Table 2. IC_{50} values were determined, as in earlier experiments, by nonlinear regression to a logistic equation in which maximal inhibition was fixed at 100% but the IC_{50} and the slope of the curve were allowed to vary. A rank order of potency of GTP > GDP > GMP > ATP was observed. Thiophosphorylated nucleotide analogs were 9- (GDPβS) to 35-fold (GTPγS) more

TABLE 3

Dependence of dissociation kinetic parameters on the duration of the prior association period

Membranes were incubated for various times (association time) with 0.4 nM p-[^{125}I] iodoclonidine. Samples were withdrawn to measure total and nonspecific binding and then unlabeled phentolamine was added (10 μM final concentration) and specific binding was measured during a 4-hr dissociation period. Data were fit to an equation specifying double-exponential dissociation: $f(t) = B_0[Ae^{-k_1 t} + (1 - A)e^{-k_2 t}]$. Results are means ± parameter standard errors, using pooled data from two independent experiments.

Association time	A	k_1	k_2
min	%	$\times 10^{-1}$ min^{-1}	$\times 10^{-3}$ min^{-1}
10	55.7 ± 4.3	4.0 ± 1.5	9.6 ± 1.9
20	48.8 ± 3.2	2.6 ± 0.6	7.6 ± 1.0
40	40.7 ± 4.1	1.9 ± 0.5	8.4 ± 1.0
90	26.4 ± 3.2	6.1 ± 7.3	8.3 ± 0.8

TABLE 4

Binding of p-[125I]iodoclonidine in various rat brain regions

Well washed membranes were obtained from various regions of the rat brain. Assays were conducted as for the pooled hippocampal plus cortical membranes described in the text but employed 4 nM p-[125I]iodoclonidine to provide an estimate of total available binding sites. The percentage of specific binding is the fraction of the total binding that is not blocked by 10 μM phentolamine. Protein concentrations were determined by a dye binding method (Bio-Rad). Results are means ± standard errors of three experiments.

Region	Specific binding	
	fmol/mg of protein	%
Cortex	268 ± 31	85 ± 1
Hippocampus	214 ± 14	82 ± 2
Striatum	87 ± 15	60 ± 2
Cerebellum	65 ± 7	54 ± 3
Diencephalon	295 ± 39	84 ± 1
Olfactory bulbs	287 ± 40	81 ± 2
Medulla-pons	124 ± 21	68 ± 3

potent than the phosphate-containing parent nucleotides. A salient feature of these competition experiments is the inability of any of the nucleotide analogs to entirely prevent the binding of the radiolabeled agonist. This is also apparent from an inspection of the slope factors, which are significantly less than unity (Table 2). The partial inhibition of p-[125I]iodoclonidine binding by the nucleotides and their analogs was also described by a model in which both the slope factor and the maximal inhibition were allowed to vary. We refer to these models as fixed and floating, respectively. Statistical testing of the appropriateness of particular models was performed using the F ratio statistic, calculated using the extra sum of squares principle described by Munson and Rodbard (21). As shown in Table 2, in all cases the floating model better described the data. Nucleotide-sensitive binding sites comprised 57 to 75% of the total sites specifically labeled by 0.4 nM p-[125I]iodoclonidine.

Kinetics of p-[125I]iodoclonidine binding. Association and dissociation experiments were performed at 25°, using 0.4 nM p-[125I]iodoclonidine, and are shown in Figs. 5 and 6, respectively. In initial experiments, association reactions were well described by a single-exponential process with a rate constant (k_{obs}) of 5.79 to 6.06 × 10^{-2} min^{-1} (values from two individual experiments). However, in subsequent experiments we focused on very early time points (15 sec to 5 min). Under these conditions, a double-exponential model provided a significantly better fit of the experimental data (three of three experiments). At asymptote, binding was 78.1 ± 21.9 fmol/mg of protein, with 37 ± 4% of this binding arising from a reaction of rate constant (k_{obs}) 0.96 ± 0.35 min^{-1} and the remainder from a slower reaction of constant 0.031 ± 0.014 min^{-1}.

Dissociation kinetics were also biexponential (Fig. 6). In these experiments, membranes were incubated for 90 min with 0.4 nM p-[125I]iodoclonidine in the presence or absence of 10 μM unlabeled phentolamine. Samples were removed for measurement of the specific binding at t_0 and then dissociation was initiated in the control membranes by the addition of phentolamine (final concentration, 10 μM). Samples were removed from both membrane preparations at various times. The data were then fit to either a single- or a double-exponential equation. In all cases, the more complex double-exponential model was found to better approximate the experimental data ($p < 0.01$). We determined (five experiments) that 30 ± 2% of the binding sites dissociate rapidly (k_1 = 0.32 ± 0.05 min^{-1}), with the remainder dissociating 50-fold more slowly (k_2 = 0.0061 ± 0.0008 min^{-1}). In one experiment, 10 μM epinephrine was used to initiate dissociation. Again, dissociation was biexponential, with 26% of the sites dissociating rapidly, with rate constants of 0.28 min^{-1} and 0.0059 min^{-1}, respectively. The results obtained by drug-induced dissociation were also compared with those obtained by dilution-induced dissociation. In three of four experiments, the latter paradigm gave results better described by the double-exponential model (47 ± 8% rapid, k_1 = 0.23 ± 0.20 min^{-1}, k_2 = 0.0084 ± 0.0049 min^{-1}).

The proportions, but not the kinetic constants, of the rapidly and slowly dissociating sites were found to vary as a function of the duration of the association period (Table 3). In these experiments (two experiments), dissociation was induced by the addition of phentolamine following 10, 20, 40, or 90 min of association. The rapidly dissociating site appeared to attain steady state levels of occupation by the radioligand at the earliest time point studied. Further incubation led to an increase in the measured specific binding, which was shown in the dissociation paradigm to arise from the slowly dissociating component.

Binding characteristics of p-[125I]iodoclonidine in various brain regions. Membranes were prepared from seven different regions of the rat brain, as described in Materials and Methods. Specific binding of a saturating concentration (4 nM) of the radiolabeled agonist was determined using well washed membranes obtained from each brain region. Specific binding varied from approximately 60% to 80% of total binding (Table 4). Highest levels of binding were observed in the diencephalon, closely followed by the olfactory bulbs, cortex, and hippocampus. Intermediate levels were found in the medulla-pons and low levels in the striatum and cerebellum.

Discussion

p-[125I]Iodoclonidine is a high affinity specific probe of the α_2AR present on brain membranes. Its combination of high specific activity and low propensity toward nonspecific binding will enable characterization of α_2ARs in tissues previously inaccessible due to low receptor abundance or the difficulty of obtaining sufficient membrane starting material. In addition, this ligand has proven useful in delineation of some of the receptor-ligand interactions that are unique to agonists.

Unlabeled p-iodoclonidine was able to attenuate forskolin-stimulated cAMP accumulation in SK-N-SH neuroblastoma cells to an extent equal to that achieved by the full agonist epinephrine. Because clonidine and its derivative p-aminoclonidine are partial agonists in other functional assays, it remains to be assessed whether the neuroblastoma cells possess 'spare receptors,' such that partial agonists can elicit the full physiological response. The EC_{50} values for epinephrine activation of the SK-N-SH α_2AR, as measured in the cAMP assay, were approximately 5-fold less than the IC_{50} of the agonist deduced from [3H]rauwolscine binding to brain membranes. In contrast, the EC_{50} of p-iodoclonidine was almost 7-fold higher in the functional assay than would be predicted from occupancy curves based on receptor binding. Receptor activation by both agonists required 10- (epinephrine) to 700-fold (p-iodoclonidine) higher agonist concentrations than would be predicted by occupancy curves based on p-[125I]iodoclonidine binding.

p-[125I]Iodoclonidine binding to well washed brain membranes was to a single class of binding sites, inasmuch as transformation of saturation binding data by the method of Scatchard (22) resulted in a straight line. This is in contrast to

the curvilinear Scatchard plots that are usually generated to describe agonist binding in competition experiments utilizing radiolabeled antagonists. A common explanation for curvilinear Scatchard plots is the existence of multiple noninteracting populations of agonist binding sites possessing varying affinities for the agonist and a uniform affinity for the radiolabeled antagonist. There are several reasons why the assay conditions used to measure *p*-[^{125}I]iodoclonidine would favor the detection of only the agonist binding subpopulation possessing the higher affinity. First, we employed a 100-fold range (0.1 to 10 nM) of radioligand concentrations, which apparently was sufficient to saturate the high affinity conformer but may have been insufficient to significantly occupy a subpopulation of lower affinity. Second, separation of bound from free ligand by rapid filtration would only reveal binding sites with dissociation half-times significantly greater than the time needed to collect and wash the membranes on the filters. Assuming diffusion-limited on-rates, the use of a filtration assay might preclude detection of receptor-ligand interactions with K_d values in excess of 10 nM (23). Finally, we have employed an extensive washing procedure to remove endogenous guanine nucleotides, the result of which would be to increase the proportion of high affinity sites. Consistent with this reasoning is the shallow slope of unlabeled *p*-iodoclonidine competition curves versus [^{3}H]rauwolscine and the approximately 100-fold greater IC_{50} value versus the antagonist than its K_d in direct binding experiments.

p-[^{125}I]Iodoclonidine binding was sensitive to nanomolar concentrations of a variety of α_2-adrenergic agonists and antagonists of diverse structure. Because clonidine has been reported to interact with a nonadrenergic imidazole-preferring site in the medulla (24), we extensively characterized the structural requirements for drugs to compete with *p*-[^{125}I]iodoclonidine binding to membranes prepared from the rat cerebral cortex. Although imidazoline-containing agonists and antagonists were among the most potent competitors for binding, the presence of this group was not necessary for potency. For example, catecholamines were able to only partially inhibit [^{3}H]clonidine binding to the medullary site (24), but in our experiments epinephrine and norepinephrine were potent and complete competitors of *p*-[^{125}I]iodoclonidine binding. Another distinction is the finding that the imidazole-containing H_2 antagonist cimetidine is a potent ligand at the medullary imidazole binding site (24), whereas cimetidine (10 μM) had no effect on *p*-[^{125}I]iodoclonidine binding. Finally, the α_1-selective stereoisomer of yohimbine, corynanthine, was almost 500-fold less potent than yohimbine in our experiments, whereas both are equipotent at the imidazole binding site (24).

Yohimbine and rauwolscine exhibited IC_{50} values that were at least 1 order of magnitude greater than those obtained via competition with radiolabeled antagonists or by direct binding with the respective radiolabeled compounds (14). Our results do, however, agree with values reported for antagonist competition with [^{3}H]clonidine (24) and [^{3}H]UK 14,304 binding (25). One explanation for these results is that the *p*-[^{125}I]iodoclonidine recognition site may be located on a different protein than the α_2AR detected by [^{3}H]rauwolscine and [^{3}H]yohimbine. We have no data to support this hypothesis and, in fact, the agonist pharmacology is as expected for an α_2AR. Instead, our results indicate that the pharmacophore for agonist and antagonist ligands is not identical. Agonists are, thus, more potent at competing for radiolabeled agonist binding, with antagonists displaying an advantage at antagonist binding sites. Supporting this hypothesis are examples of reciprocal modulation of agonist and antagonist binding affinity. For example, monovalent cations such as sodium increase antagonist affinity and decrease agonist affinity (Ref. 26 and present study). In contrast, divalent cations such as magnesium increase agonist binding but decrease antagonist binding (Ref. 25 and the present study).

As expected for a radiolabeled agonist, the binding of *p*-[^{125}I]iodoclonidine was sensitive to guanine nucleotides. Triphosphate-containing nucleotides or analogs were more potent than the diphosphate-containing homologs. Surprisingly, none of the nucleotides or analogs could inhibit greater than 75% of the binding. There did not appear to be any relationship between the maximal fraction of nucleotide-sensitive binding revealed by diphosphate- or triphosphate-containing nucleotides and their analogs and their reported efficacy in stimulating adenylate cyclase (Ref. 27 and references therein). Rather, our data suggest that, under the conditions of our assays, a fraction (30%) of the α_2ARs in the brain membrane preparation were insensitive to guanine nucleotides. Alternatively, the brain membrane preparation used in our experiments may contain GTP-binding proteins with differing affinities for the nucleotide, with those of low affinity not achieving saturation under our experimental conditions.

Bylund (14) has presented evidence for pharmacological heterogeneity of α_2ARs, based in part on the sensitivity of the putative receptor subtypes to prazosin. We observed that slopes of prazosin competition curves were significantly less than unity, perhaps indicating a subpopulation of prazosin-sensitive α_2ARs (e.g., α_{2b} by the classification scheme of Bylund in Ref. 14) that were labeled by *p*-[^{125}I]iodoclonidine in the rat cerebral cortex-hippocampus homogenate.

This apparent heterogeneity of brain α_2ARs is also reflected in the complex association and dissociation kinetics of bound *p*-[^{125}I]iodoclonidine. Using 0.4 nM *p*-[^{125}I]iodoclonidine, roughly 30% of the ligand bound rapidly, with the remaining fraction binding 30-fold more slowly. Dissociation was also biexponential, with 30% dissociating rapidly, with a half-time of 2.2 min, and the remainder dissociating with a half-time of 114 min. The proportion of the rapidly dissociating binding sites was dependent on the length of the association time, with shorter incubation times favoring the labeling of this component. These kinetic states may arise from a heterogeneity of the binding protein, interaction of the binding protein with a second protein (e.g., a GTP-binding protein), or differing physical disposition and, hence, accessibility to the radioligand of α_2AR pools in the membrane homogenate (e.g., inside versus outside of vesicles).

Multiphasic association and dissociation kinetics have been reported by others measuring radiolabeled α_2-agonist binding (25, 28, 29). Neubig *et al.* (28), on the basis of kinetic and equilibrium binding studies, postulate the existence of three distinct binding sites for α_2-adrenergic agonists. In their model, approximately one third of the α_2ARs bound agonist with low affinity and did not couple to a GTP-binding protein, one third were coupled to a GTP-binding protein before binding the agonist, and one third became coupled to the GTP-binding protein subsequent to agonist occupation. Thus, in control membranes, saturation binding studies using [^{3}H]UK 14,304 revealed two binding sites of differing affinity for the agonist. However, in the presence of the GTP analog Gpp(NH)p, only

a fraction of the total binding was observed with affinity and abundance like those expected for the low affinity site present on control membrane preparations (28). This suggests that the low affinity subpopulation is GTP insensitive, whereas the GTP-sensitive high affinity agonist binding subpopulation is converted in the presence of the nucleotide to an affinity state that is not trapped on the filter. In contrast, we have only observed a single class of p-[125I]iodoclonidine binding sites in saturation studies with brain membranes. We do, however, find evidence for the existence of a subpopulation of GTP-insensitive agonist binding sites in brain membranes, based on the inability of a variety of guanine nucleotides and analogs to fully prevent the binding of p-[125I]iodoclonidine. The fraction of the total brain membrane binding sites we observe to be sensitive to guanine nucleotides (approximately 70%) is similar to the GTP-sensitive fraction observed by Neubig *et al.* (28) in platelet membranes.

Kinetic data from association experiments gave results consistent with association to a heterogeneous class of binding sites. Moreover, dissociation experiments initiated during various phases of the association period suggest that there is a very rapid filling of a rapidly dissociating component, followed by a slow loading onto a slowly dissociating component. Thus, circumstantial evidence suggests that the rapidly associating component is identical to the rapidly dissociating component. Based on this assumption, the kinetically derived K_d was calculated for the two sites. For each site, we calculated k'_{on} as $(k_{obs} + k_2)L$, where k'_{on} is the pseudo-first-order rate constant, k_{obs} is the observed association rate constant, k_2 is the dissociation rate constant for that site, and L is the radioligand concentration. Propagated error for the two ratios (k_{off}/k_{on}) was calculated using standard statistical methods. The K_d values (mean ± variance) were 0.20 ± 0.10 nM and 0.10 ± 0.05 nM for the fast on-fast off and slow on-slow off sites, respectively. These values are not significantly different from each other. Therefore, it is not surprising that we obtained linear Scatchard plots in saturation binding experiments conducted at equilibrium, because the complexity in the on-rates compensates for the observed complexity in the off-rates. The magnitude of the kinetically derived K_d (0.1 to 0.2 nM) is also similar to that calculated from equilibrium binding experiments (0.5 nM).

p-[125I]Iodoclonidine binding to various brain regions paralleled the density of α_2ARs observed in autoradiographic studies with [3H]idazoxan (30) or with [3H]clonidine (31). These authors compared autoradiographic density of [3H]idazoxan binding with that of [3H]rauwolscine binding. There appear to be substantial discrepancies in the binding of these two ligands (the magnitude of idazoxan binding is generally greater than that of rauwolscine binding), although the authors caution that direct comparison of densities is not valid, because these assays were not conducted under conditions that would provide estimates of the B_{max} value (30). In this regard, it should be noted that [3H]idazoxan is capable of labeling a nonadrenergic site (32). The pharmacology of this site is unlike that described above for the imidazole binding site, because this site can apparently discriminate between clonidine (inactive) and the clonidine analog UK 14,304 (potent). These characteristics, coupled with the ineffectiveness of catecholamines in competing for this nonadrenergic site, argue that the site labeled by p-[125I]iodoclonidine in our experiments using cerebral cortical and hippocampal membranes is significantly different from the nonadrenergic [3H]idazoxan binding site. However, because we have not attempted a pharmacological characterization of p-[125I]iodoclonidine binding sites in other brain regions (e.g., the medulla), we cannot conclude that the binding of the radioligand in these brain regions is similarly restricted to α_2ARs.

In our experiments, the radiolabeled agonist demonstrated a constant low level of nonspecific binding across all brain regions, suggesting little tendency of this hydrophilic ligand to partition into brain white matter. This combination of low nonspecific binding and high specific activity should prove useful in further studies characterizing α_2ARs present on cultured cells and in discrete brain regions. Indeed, preliminary studies have demonstrated that this ligand is an excellent probe for brain α_2ARs in autoradiographic studies.[1]

In conclusion, p-[125I]iodoclonidine is a useful probe of brain α_2ARs. This ligand binds in a saturable and reversible manner to the brain α_2AR and possesses subnanomolar affinity for its binding site. The ligand does not bind to α_1ARs and exhibits very low levels of nonspecific binding. p-[125I]Iodoclonidine should prove very useful in future studies of α_2-adrenergic structure-activity relationships and in delineation of some of the characteristics of α_2-adrenergic binding that are specific to agonists.

[1] J. A. Miller. Quantitative autoradiographic localization of α-adrenergic receptors in the rat brain and spinal cord using the novel radioligand [125I]p-iodoclonidine. Manuscript in preparation.

Acknowledgments

The authors wish to thank Dr. Michael G. Palfreyman, Dr. Jules Freedman, and Dr. Jerry A. Miller (all of Merrell Dow Research Institute, Cincinnati, OH), Dr. Lee E. Limbird (Vanderbilt University, Nashville, TN), and Dr. Henry I. Yamamura (University of Arizona, Tucson, AZ) for their helpful suggestions and for critically reading this manuscript.

References

1. Limbird, L. E. Receptors linked to inhibition of adenylate cyclase: additional signaling mechanisms. *FASEB J.* **2**:2686–2695 (1988).
2. Sabol, S. K., and M. Nirenberg. Regulation of adenylate cyclase of neuroblastoma × glioma hybrid cells by *a* α-adrenergic receptors. I. Inhibition of adenylate cyclase mediated by α-receptors. *J. Biol. Chem.* **254**:1913–1920 (1979).
3. Kitamura, Y., Y. Nomura, and T. Segawa. Possible involvement of inhibitory GTP binding regulatory protein in α_2-adrenoceptor-mediated inhibition of adenylate cyclase activity in cerebral cortical membranes of rats. *J. Neurochem.* **45**:1504–1508 (1985).
4. Duman, R. S., and S. J. Enna. A procedure for measuring α_2-adrenergic receptor-mediated inhibition of cyclic AMP accumulation in rat brain slices. *Brain Res.* **384**:391–394 (1986).
5. Baron, B. M., and B. W. Siegel. *Alpha*$_2$-adrenergic and muscarinic cholinergic receptors have opposing actions on cyclic AMP levels in SK-N-SH human neuroblastoma cells. *J. Neurochem.* **53**:602–609 (1989).
6. Pilc, A., and S. J. Enna. Antidepressant administration has a differential effect on rat brain α_2-adrenoceptor sensitivity to agonists and antagonists. *Eur. J. Pharmacol.* **132**:277–282 (1986).
7. Fraser, C. M., S. Arakawa, W. R. McCombie, and J. C. Venter. Cloning, sequence analysis, and permanent expression of a human α_2-adrenergic receptor in Chinese hamster ovary cells. *J. Biol. Chem.* **264**:11754–11761 (1989).
8. Johnston, H., H. Majewski, and I. F. Musgrave. Involvement of cyclic nucleotides in prejunctional modulation of noradrenaline release in mouse atria. *Br. J. Pharmacol.* **91**:773–781 (1987).
9. Musgrave, I., P. Marley, and H. Majewski. Pertussis toxin does not attenuate α_2-adrenoceptor mediated inhibition of noradrenaline release in mouse atria. *Naunyn-Schmiedeberg's Arch. Pharmacol.* **336**:280–286 (1987).
10. Ong, M. L., S. G. Ball, and P. F. T. Vaughan. The effect of cyclic AMP on the inhibition of noradrenaline release, from rat occipital cortex tissue chops, by clonidine. *Biochem. Soc. Trans.* **16**:311–312 (1988).
11. Kobilka, B. K., H. Matsui, T. S. Kobilka, T. L. Yang-Feng, U. Francke, M. G. Caron, R. J. Lefkowitz, and J. W. Regan. Cloning, sequencing, and expression of the gene coding for the human platelet α_2-adrenergic receptor. *Science* (*Washington D. C.*) **238**:650–656 (1987).
12. Weinshank, R. L., H. M. Lichtblau, and P. R. Hartig. Cloning of a new G-protein-coupled receptor homologous to the *alpah*-2 adrenergic receptor. *Soc. Neurosci. Abstr.* **15**:170 (1989).

13. Regan, J. W., T. S. Kobilka, T. L. Yang-Feng, M. G. Caron, R. J. Lefkowitz, and B. K. Kobilka. Cloning and expression of a human kidney cDNA for an α_2-adrenergic receptor subtype. *Proc. Natl. Acad. Sci. USA* **85**:6301–6305 (1988).
14. Bylund, D. B. Heterogeneity of *alpha*-2 adrenergic receptors. *Pharmacol. Biochem. Behav.* **22**:825–843 (1985).
15. de Jonge, A., P. N. Santing, P. B. M. Timmermans, and P. A. van Zwieten. A comparison of peripheral pre- and postsynaptic α_2-adrenoceptors using metasubstituted imidazolidines. *J. Auton. Pharmacol.* **1**:377–383 (1981).
16. Ruffolo, R. R., A. C. Sulpizio, A. J. Nichols, R. M. DeMarinis, and J. P. Heible. Pharmacologic differentiation between pre- and postjunctional α_2-adrenoceptors by SK & F 104078. *Naunyn-Schmiedeberg's Arch. Pharmacol* **336**:415–418 (1987).
17. Van Dort, M., R. Neubig, and R. E. Counsell. Radioiodinated *p*-iodoclonidine: a high-affinity probe for the α_2-adrenergic receptor. *J. Med. Chem.* **30**:1241–1244 (1987).
18. Neubig, R. R., and O. Szamraj. Large-scale purification of α_2-adrenergic receptor-enriched membranes from human platelets: persistent association of guanine nucleotides with nonpurified membranes. *Biochim. Biophys. Acta* **854**:67–76 (1986).
19. Baron, B. M., M. W. Dudley, D. R. McCarty, F. P. Miller, I. J. Reynolds, and C. J. Schmidt. Guanine nucleotides are competitive inhibitors of *N*-methyl-D-aspartate at its receptor site both *in vitro* and *in vivo*. *J. Pharmacol. Exp. Ther.* **250**:162–169 (1989).
20. Cheung, Y., D.B. Barnett, and S. R. Nahorski. [^{3}H]Rauwolscine and [^{3}H] yohimbine binding to rat cerebral and human platelet membranes: possible heterogeneity of α_2-adrenoceptors. *Eur. J. Pharmacol.* **84**:79–85 (1982).
21. Munson, P. J., and D. Rodbard. LIGAND: a versatile computerized approach for characterization of ligand-binding systems. *Anal. Biochem.* **107**:220–239 (1980).
22. Scatchard, G. The attraction of proteins for small molecules and ions. *Ann. N. Y. Acad. Sci.* **51**:660–672 (1949).
23. Yamamura, H. I., S. J. Enna, and M. Kuhar. *Neurotransmitter Receptor Binding*, Ed. 1. Raven Press, New York (1978).
24. Ernsberger, P., M. P. Meeley, J. J. Mann, and D. J. Reis. Clonidine binds to imidazole binding sites as well as α_2-adrenoceptors in the ventrolateral medulla. *Eur. J. Pharmacol.* **134**:1–13 (1987).
25. Loftus, D. J., J. M. Stolik, and D. C. U'Pritchard. Binding of the imidazoline UK-14,304, a putative full α_2-adrenoceptor agonist, to rat cerebral cortex membranes. *Life Sci.* **35**:61–69 (1984).
26. Limbird, L. E., J. L. Speck, and S. K. Smith. Sodium ion modulates agonist and antagonist interactions with the human platelet *alpha*$_2$-adrenergic receptor in membrane and solubilized preparations. *Mol. Pharmacol.* **21**:609–617 (1982).
27. Eckstein, F. Guanosine 5-*O*-(2-thiodiphosphate): an inhibitor of adenylate cyclase stimulation by guanine nucleotides and fluoride ions. *J. Biol. Chem.* **254**:9829–9834 (1979).
28. Neubig, R. R., R. D. Gantzos, and W. J. Thomsen. Mechanism of agonist and antagonist binding to α_2-adrenergic receptors: evidence for a precoupled receptor-guanine nucleotide protein complex. *Biochemistry* **27**:2374–2384 (1988).
29. Paris, H., J. Galitzky, and M. Senard. Interactions of full and partial agonists with HT29 cell α_2-adrenoceptor: comparative study of [^{3}H]UK-14,304 and [^{3}H]clonidine binding. *J. Pharmacol. Exp. Ther.* **35**:345–354 (1989).
30. Boyajian, C. L., S. E. Loughlin, and F. M. Leslie. Anatomical evidence for *alpha*-2 adrenoceptor heterogeneity: differential autoradiographic distributions of [^{3}H]rauwolscine and [^{3}H]idazoxan in rat brain. *J. Pharmacol. Exp. Ther.* **241**:1079–1091 (1987).
31. Nock, B., A. E. Johnson, H. H. Feder, and B. S. McEwen. Tritium-sensitive film autoradiography of guinea pig brain α_2-noradrenergic receptors. *Brain Res.* **336**:148–152 (1985).
32. Michel, M. C., O. Brodde, B. Schnepl, J. Behrendt, R. Tschada, H. J. Motulsky, and P. A. Insel. [^{3}H]Idazoxan and some other α_2-adrenergic drugs also bind with high affinity to a nonadrenergic site. *Mol. Pharmacol.* **35**:324–330 (1989).

Send reprint requests to: Bruce M. Baron, Merrell Dow Research Institute, 2110 E. Galbraith Rd., Cincinnati, OH 45215.